Plasma Sci. Technol. **24** (2022) 025402 (7pp) https://doi.org/10.1088/2058-6272/ac3971

Spatiotemporal control of femtosecond laser filament-triggered discharge and its application in diagnosing gas flow fields

Zhifeng ZHU (朱志峰)[1], **Bo LI** (李博)[1], **Qiang GAO** (高强)[1], **Jiajian ZHU** (朱家健)[2] **and Zhongshan LI** (李中山)[1,3]

[1] State Key Laboratory of Engines, Tianjin University, Tianjin 300350, People's Republic of China
[2] College of Aerospace Science and Engineering, National University of Defense Technology, Changsha 410073, People's Republic of China
[3] Division of Combustion Physics, Lund University, Lund SE-22100, Sweden

E-mail: qiang.gao@tju.edu.cn

Received 22 July 2021, revised 11 November 2021
Accepted for publication 12 November 2021
Published 17 February 2022

Abstract

Precise control of the discharge in space and time is of great significance for better applications of discharge plasma. Here, we used a femtosecond laser filament to trigger and guide a high-voltage DC pulse discharge to achieve spatiotemporal control of the discharge plasma. In space, the discharge plasma is distributed strictly along the channel generated by the femtosecond laser filament. The breakdown voltage threshold is reduced, and the discharge length is extended. In time, the electrical parameters such as the electrode voltage and the electrode gap affect discharge delay time and jitter. By optimizing the parameters, we can achieve sub-nanosecond jitter of the discharge. Based on the spatiotemporal control of the discharge, we applied filament-triggered discharge for one-dimensional composition measurements of the gas flow field. Besides, the technique shows great potential in studying the spatiotemporal evolution of discharge plasma.

Keywords: femtosecond laser, filamentation, high voltage discharge, discharge plasma, spectrum

(Some figures may appear in colour only in the online journal)

1. Introduction

Atmospheric pressure gas discharges have been used in widespread applications, including spark gap switch [1], combustion ignition [2, 3], material preparation [4, 5], environmental pollution control [6], and biomedicine [7]. A stable discharge is an essential basis for its applications. However, the discharge inception in air relies on the acceleration of free electrons in the local electric field and the subsequent electron avalanches [8–10]. Breakdown starts with the development of a high conductive channel between both electrodes, which is commonly formed by streamers or leaders [11, 12]. Generally, positive streamers attain a characteristically ragged, zigzagged, and narrow shape [13]. The propagation path of discharge leaders is usually twisted [14, 15]. The discharge mechanism leads to the spatiotemporal instability of the discharge, which imposes a potential limitation on the practical applications of discharge plasma. Hence, precise control of the discharge in space and time is of great importance, for which, triggering and controlling discharges by a laser is a promising method.

In a laser-triggered discharge, there are essentially three methods [16, 17]. First, the laser beam is focused on the surface of one of the electrodes to create a high degree of ionization. Second, the laser beam is focused on the electrode gap to break down the gas. Third, the laser creates a low ionization plasma in a long gap between the electrodes. The first two methods typically use a nanosecond (ns) laser, while the last one uses a femtosecond (fs) laser.

In most cases, the plasma produced by an ns laser can efficiently trigger the discharge. However, due to the limited plasma volume, it is not suitable for triggering and guiding

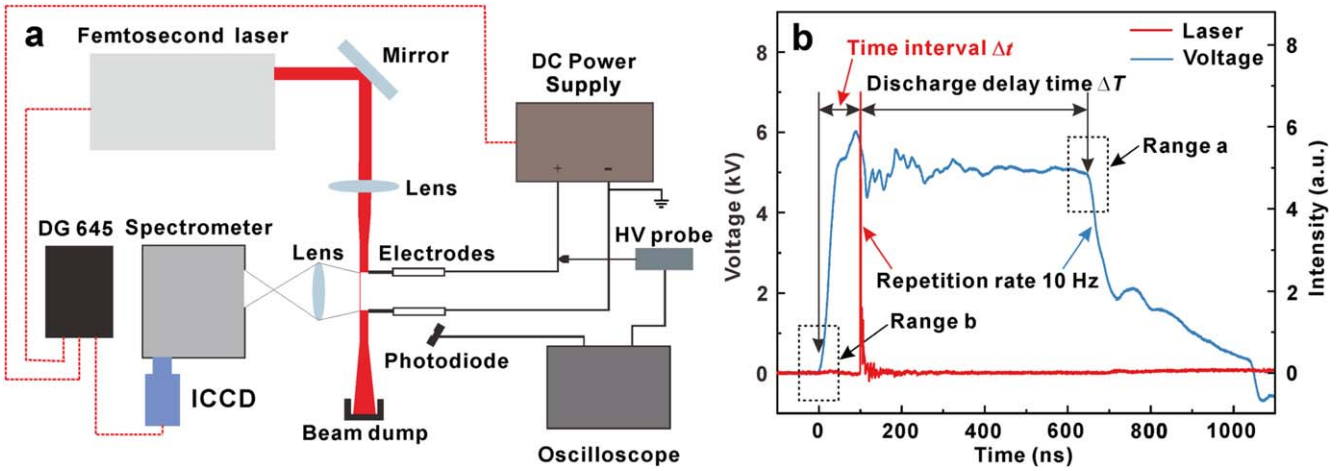

Figure 1. (a) Experimental setup, (b) time sequence waveforms of voltage and scattering signal of fs laser.

long-distance discharges. Femtosecond laser filamentation is a dynamically self-guided propagation region where self-focusing by the Kerr effect and defocusing by the generated plasma result in a continuous extended length of low-density plasma [18]. The filament is a weak conductive channel with a diameter on the order of a hundred microns and a length longer than the Rayleigh length [19], which can trigger and guide long-distance discharges.

Early works about the control of the discharge by the fs filament have been done. In spatial control, the discharge arc propagates along the fs filament [20–24]. In addition, the electric discharges can be effectively manipulated along a complex predefined path by using judiciously shaped laser radiation [25]. In temporal control, different parameters [26, 27], such as laser energy, and electrode voltage, have a significant impact on the discharge delay time and jitter. A higher electrode voltage and laser energy result in a short discharge delay time and jitter [28, 29]. The discharge jitter can be controlled to be within sub-nanoseconds [30, 31]. Thus, fs laser filament-triggered discharge shows great potential for many applications [32, 33], such as guiding lightning [34–36], fast switches for high-voltage connection [37, 38], and reconfigurable RF antennas [39, 40].

Due to the luminescence characteristics of discharge plasma, we believe that the discharge triggered by the fs laser filament also has excellent potential for one-dimensional composition measurements. The accuracy of spatial and temporal control of the discharge plasma affects the spatial and temporal resolution of one-dimensional composition measurements. So, it is necessary to study the spatial and temporal control of the discharge triggered by an fs laser filament, which is the basis of its applications.

This paper presents the results of an experimental investigation of the spatial and temporal control of the discharge triggered by the fs laser filament. In spatial control, the discharge path and discharge length triggered by the fs laser filament were investigated. In temporal control, the discharge delay time and the jitter were found to be highly dependent on several parameters such as the time interval between the laser pulse and the voltage pulse, the electrode voltage, and the electrode gap. The discharge plasma is distributed strictly along the channel generated by the fs laser filament. The discharge jitter can be controlled to be within sub-nanoseconds. Finally, based on the spatiotemporal control of the discharge plasma, we employed the discharge plasma in a free gas jet of SF_6. The one-dimensional temporally and spatially resolved spectra of the discharge plasma in SF_6 were measured. The results demonstrated that fs laser filament-triggered discharge could be used for online one-dimensional composition measurements of gas flow fields. Femtosecond laser filament-triggered discharge is also helpful to study the spatiotemporal evolution of discharge plasma.

2. Experimental setup

Figure 1(a) illustrates the experimental setup. The fs laser source was the fundamental output from an fs Ti:sapphire laser (Spitfire Ace, Spectra-Physics), 800 nm in wavelength, 45 fs in pulse duration, and 6 mJ in pulse energy. The repetition rate of the fs laser in the experiment was 10 Hz. The laser was focused by a spherical lens ($f = 500$ mm), and a visible fs laser filament was formed.

Two conical electrodes connected to the positive and ground terminals, respectively, of a high-voltage DC pulse power supply (HVP-20, Xi'an Smart Maple Electronic Technology) were placed close to the filament. The distance between the tip of the electrodes and the filament path is about 0.2 mm. The discharge gap could be adjusted using a translation table. The power supply output is a square wave voltage pulse with 10 Hz in pulse frequency, 1 μs in pulse width, and 50 ns in both rising and falling time. The voltage amplitude ranges from 0 to 20 kV.

The time interval between the laser pulse and the voltage pulse was controlled by a digital pulse generator (DG 645, Stanford Research Systems). The scattering signal of the fs laser was detected by a photodiode (DET10A/M, THORLABS), and the voltage between the electrodes was detected by a voltage probe (P6015A, Tektronix). The waveforms were simultaneously recorded by a 600 MHz oscilloscope (WaveRunner

606zi, Teledyne Lecroy). Figure 1(b) shows the time sequence waveforms of the voltage and the scattering signal of the fs laser. The extreme points of the waveforms can be found by mathematical derivation (judged by the first and second derivatives). For the voltage pulse, the last time of the maximum near the rapid voltage drop (range a in figure 1(b)) is considered as the moment of discharge breakdown. The last time of the minimum (range b in figure 1(b)) near the voltage rise is considered as the moment of voltage rise. The range is generally 100 ns. The arrival time of the laser pulse can be obtained using the same method. After that, the voltage rise is defined as zero. The time delay (difference in time) between the voltage rise and the laser pulse can be obtained, which is defined as the time interval Δt. The time delay between the laser pulse and the discharge breakdown can be obtained, which is defined as the discharge delay time ΔT. The standard deviation of five measurements of the discharge delay time is defined as the discharge jitter. For example, $\Delta t = 100$ ns, and $\Delta T = 550$ ns are shown in figure 1(b).

Finally, we placed the spatiotemporal controlled discharge plasma into a free gas jet of SF_6 surrounded by air. The optical emission spectra of the plasma were measured using a spectrometer (Acton 2300i, Princeton Instrument) combined with an ICCD camera (PIMAX3, Princeton Instrument). The emission from the discharge plasma was imaged onto the entrance slit, which was parallel with the filament to allow a spatially resolved measurement along the laser direction. All experiments were conducted at an ambient temperature of ~300 K.

3. Results and discussions

3.1. The spatial and temporal control of the discharge

The propagation path of free electric discharges in the atmosphere is distorted and unpredictable. Figures 2(a) and (b) show the free discharges between the two electrodes. The voltage was 12 kV, and the electrode gap was 8 mm. We photographed the spatial paths of the electric discharges 30 times consecutively using an SLR camera and calculated the offset distance Δx of the discharge channel. The offset distance Δx is defined as the maximum distance between the discharge channel and the axis of the two electrode connections. When the discharge channel is offset upwards, the offset distance is defined as a positive value. The absolute value of the offset distance is defined as ΔX. The offset distance of the electric discharges is shown in figure 2(e). The offset distance Δx has strong randomness. The average offset distance Δx is about -0.19 mm, and the maximum Δx is about 1.5 mm. The average of ΔX is about 0.74 mm. Figure 2(c) shows the fs laser filamentation. The laser pulse ionizes the gases in the filament and generates a channel of low conductivity. Triggered by this channel, the discharge strictly propagates along the channel, as shown in figure 2(d). In this case, almost no offset was observed with the spatial resolution of about 35 μm.

The gas number density in the filament is reduced by the laser heating effect [41], which lowers the threshold of the breakdown voltage between the two electrodes. Therefore, the discharge arc length can be extended. Figure 3 shows the maximum arc length at different electrode voltages. The arc length is the distance between the electrodes, as the discharge triggered by the fs laser filament is spatially straight. The length can be approximately 32 mm at a voltage of 12 kV and laser energy of 6 mJ/pulse.

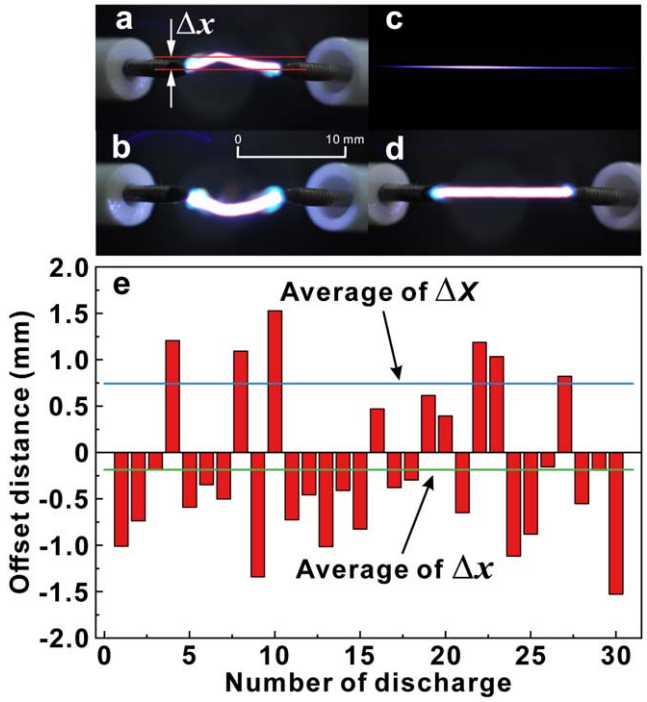

Figure 2. (a) and (b) Electric discharges, (c) femtosecond laser filament, (d) filament-triggered discharge, (e) offset distance of electric discharges.

We further measured the minimum applied voltage for the electric discharge and the filament-triggered discharge at different electrode gaps. Then the breakdown voltage was calculated. The results are shown in figure 3(b). The minimum applied voltage increases linearly with the electrode gap increases. The breakdown voltage with filament is about 4 kV cm^{-1}, roughly one-fourth of that without filament, i.e. about 16 kV cm^{-1}. The laser filament decreases the breakdown voltage by a factor of about 4. Thus, triggered by a fs filament, a discharge plasma can be obtained where the discharge arc is distributed along the filament, and the discharge arc length can be extended.

The discharge delay time and the jitter are essential parameters to characterize the stability of the discharge in time. These two essential parameters are evaluated here. For filament-triggered discharge, the filament generated before or during the application of the electric field can successfully trigger and guide the discharge. We found that the time interval between the filament and the electrode voltage affects the stability of the discharge.

Figure 4(a) shows the discharge delay time at different time intervals with an electrode gap of 10 mm and a voltage of 5 kV. As the time interval Δt gradually increases, the discharge delay time ΔT decreases. When $\Delta t < 0$, the time

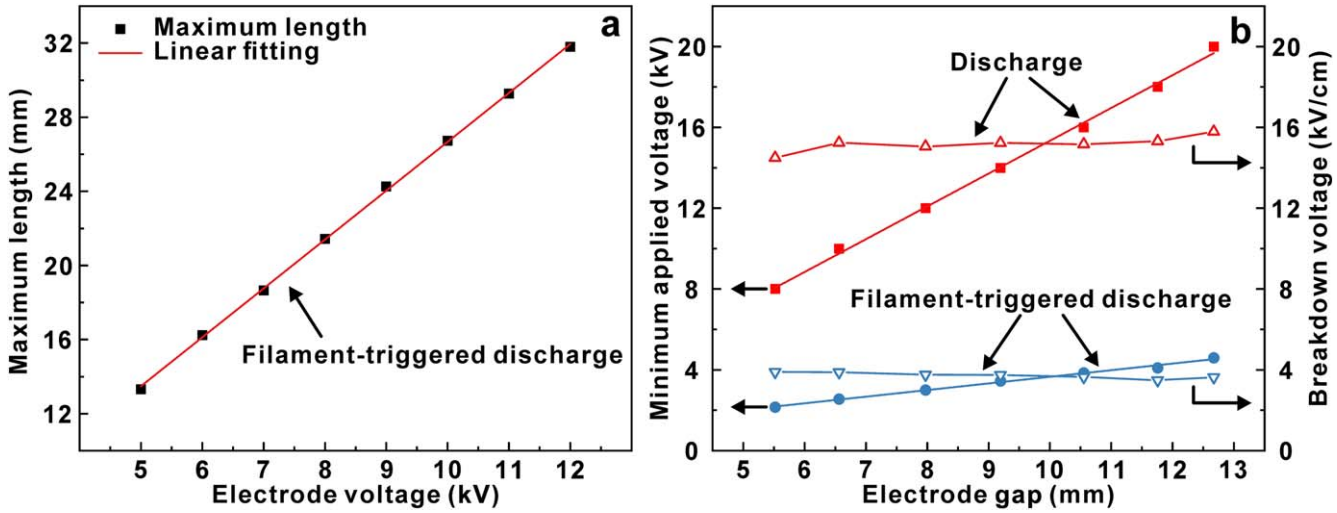

Figure 3. (a) Maximum length versus electrode voltage, (b) minimum applied voltage and breakdown voltage at different electrode gaps.

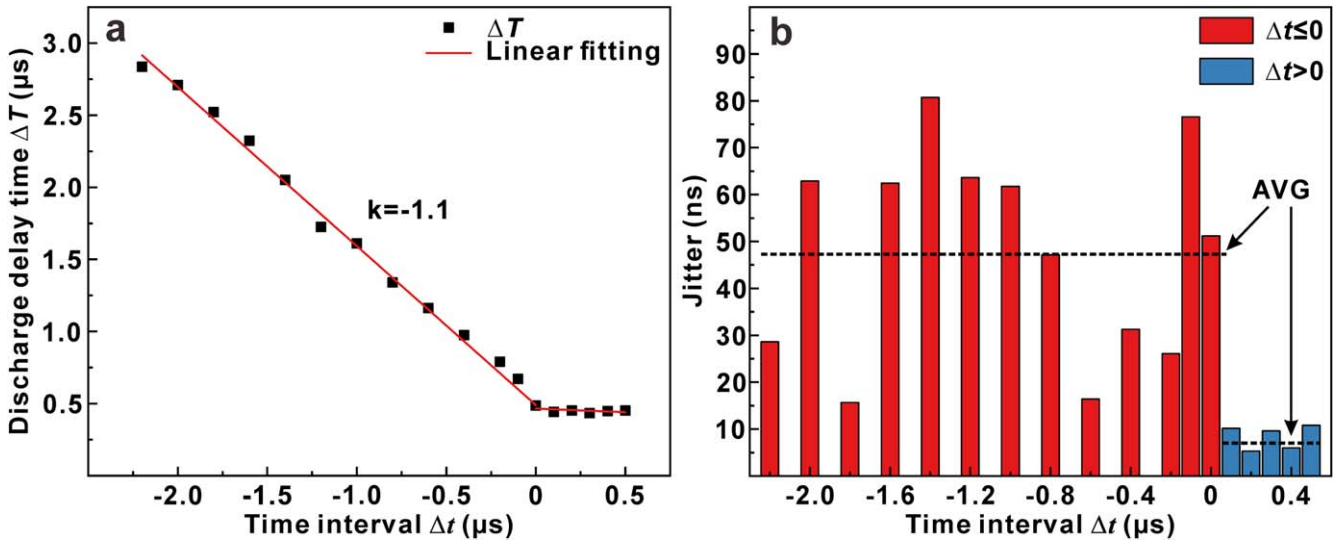

Figure 4. (a) Discharge delay time ΔT at different time intervals Δt at an applied voltage of 5 kV, (b) discharge jitter at different time intervals at an applied voltage of 5 kV.

interval and the discharge delay time are linearly correlated. The slope of the fitting line is -1.1, which is close to 1. The minimum discharge delay time is reached when the time interval is 0. When $\Delta t > 0$, the discharge delay time is almost unchanged at about 500 ns. The filament will not successfully trigger and guide the discharge with larger or smaller time intervals. This curve also shows that the discharge breakdown inception can be controlled by simply adjusting the time interval Δt.

The electron density of the fs laser filament drops rapidly after several nanoseconds [35, 42]. However, the filament generated 2 μs before the electric field can still successfully trigger and guide the discharge. This phenomenon proves that the low-density channel generated by the fs laser filament plays a key role in triggering the discharge. The existence of the minimum discharge delay time indicates that there is a threshold reduced electric field defined as E/N (where N is the gas density). This field is about 30 kV cm^{-1}. The gas density depletion increases with the laser energy deposited.

We further measured the jitter of the discharge delay time at different time intervals, as shown in figure 4(b). The jitter is the standard deviation of five measurements of the discharge delay time. The average jitter is around 8 ns when $\Delta t > 0$. It increases to around 48 ns when $\Delta t < 0$. When the filament is generated in the presence of an external field, the electrons generated by multiphoton ionization of the fs laser will produce a significant Joule heating in the filament and increase the heating effect of the filament strongly [23]. It reduces the gas density in the filament. The stability of the discharge will be improved. In addition, the electrons in the filament may act as seed electrons for the discharge and improve the stability of the discharge. Therefore, it is preferable to directly generate the fs laser filament in an electric field to reduce the discharge jitter.

To optimize the discharge control, we investigated the effect of the electrode voltage on the discharge stability.

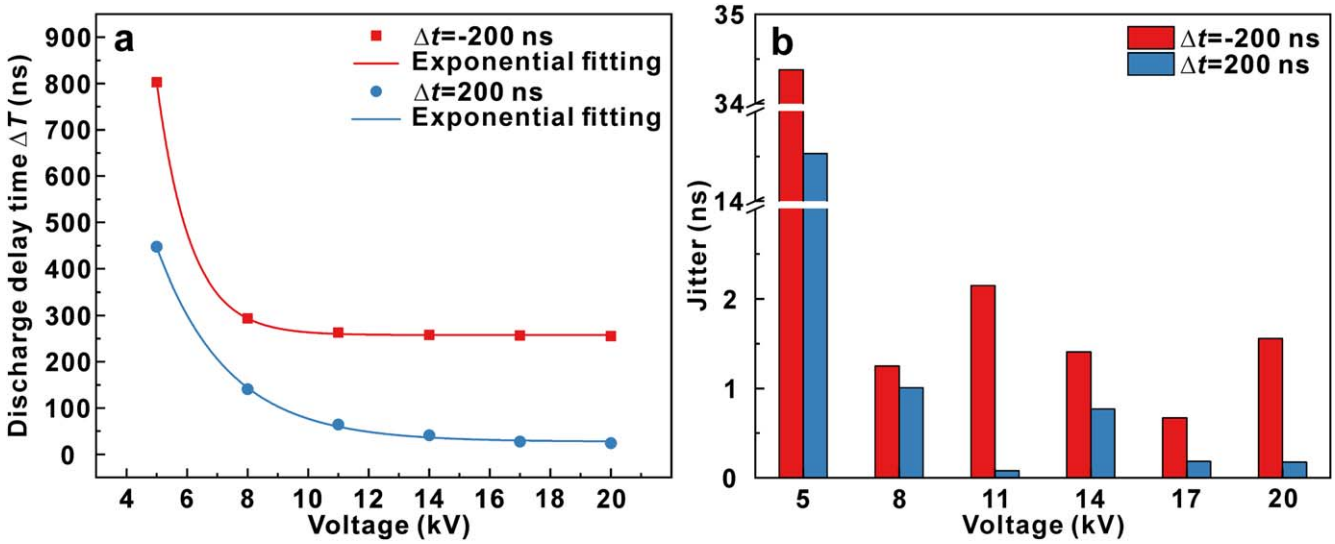

Figure 5. Discharge delay time ΔT (a) and jitter (b) at different voltages.

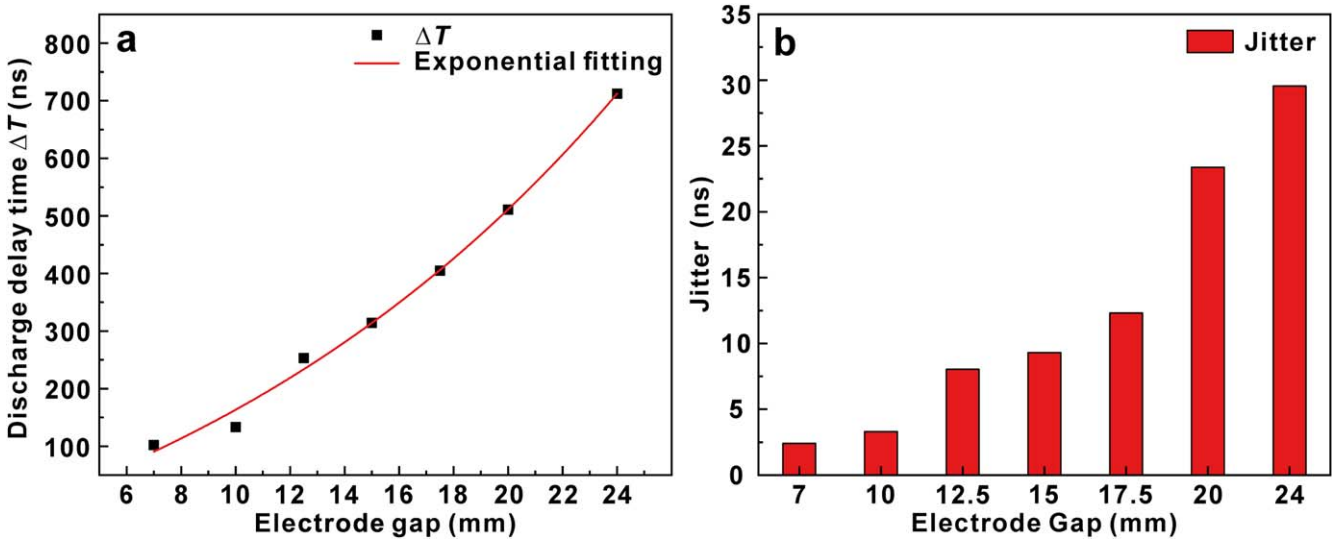

Figure 6. Discharge delay time ΔT (a) and jitter (b) at different gaps.

Figure 5(a) shows the discharge delay time at different voltages. The electrode gap was set to 10 mm. The time interval was set to 200 and −200 ns. The horizontal coordinate is the voltage, and the vertical coordinate is the discharge delay time. The discharge delay time decreases with the increase of the discharge voltage. This trend is in agreement with the similar measurements in previous research [31]. The discharge delay time decreases faster at a time interval of −200 ns. The minimum discharge delay time at a time interval of −200 ns is larger than 200 ns. Figure 5(b) shows the jitter at different voltages. Overall, the jitter at the time interval of 200 ns is smaller than that at −200 ns. This is consistent with the results in figure 4(b). A shorter discharge delay time can be obtained at a higher voltage. The jitter on the order of nanoseconds or even sub-nanoseconds can be obtained.

The discharge delay time and the jitter at different gaps were measured and shown in figures 6(a) and (b), respectively. The electrode voltage was 8 kV. The time interval was 200 ns. The discharge delay time and the jitter increase exponentially as the gap increases. Thus, there is a trade-off between the discharge plasma length and the discharge stability. In other words, for one-dimensional composition measurements, there is a trade-off between the measurable spatial range and the temporal resolution.

After the discussion above, we know that the precise control of the discharge in time can be accomplished by optimizing electrical parameters, such as the electrode gap, the electrode voltage, and the time interval between the fs laser filament and the electric field. For example, with a voltage of 20 kV, a time interval of 200 ns, and an electrode gap of 10 mm, a precisely controlled discharge with a

discharge delay time of 24 ns and discharge jitter of 175 ps can be obtained.

3.2. Application in diagnosing gas flow fields

By optimizing the electrical parameters, we can obtain a discharge plasma that is precisely controlled in time and is spatially distributed along the filament. The discharge plasma combined with optical emission spectroscopy can be applied to measure the composition of gas flow fields along one direction.

As an example, we performed a measurement investigation in sulfur hexafluoride (SF_6) gas. Sulfur hexafluoride is often used as an insulating gas in high-voltage equipment [43], since it is extremely difficult to generate breakdown in SF_6 through electric discharge. Therefore, it becomes problematic when we would like to study the evolution of the discharge plasma in SF_6. Femtosecond laser filament-triggered discharge mentioned above might help to address this issue since it can largely reduce the breakdown threshold. Meanwhile, the discharge is precisely controlled in time and is spatially distributed along the filament. Therefore, this method has significant advantages in studying the evolution of the discharge plasma in SF_6.

A glass pipe, 2.8 mm in diameter, was used for this purpose. The pipe was supplied with pure SF_6 gas (99.999% purity), and the SF_6 gas was ejected from the pipe into ambient air with a speed of 5 m s^{-1}. In the SF_6 gas near the pipe's exit, an electric discharge triggered by the fs laser filament was generated.

The optical emission spectra of the discharge plasma were measured using an imaging spectrometer with a gate width of 100 μs. The entrance slit of the spectrometer was parallel with the filament, and hence, the plasma channel, to allow spatially resolved spectral measurements along the laser propagation direction. The results are shown in figure 7. Figure 7(a) shows the image of a one-dimensionally resolved spectrum of the flow field with the SF_6 gas in the middle position and the air on both sides. Two clear flow field boundaries between the SF_6 gas and the ambient air can be observed in figure 7(a) (as indicated by two arrows), which demonstrates the ability of fs laser filament-triggered discharge to undertake one-dimensional measurements of the gas flow field.

The spectral intensities along the two white dashed lines in figure 7(a) are shown in figures 7(b) and (c), respectively. Figure 7(b) is the discharge plasma spectrum of SF_6. A large number of F atoms and S ions appear in the SF_6 discharge plasma spectrum, with F atoms mainly at 600–800 nm and S ions at 500–550 nm. The F atoms and S ions are generated by the collisional dissociation of SF_6 molecules. The discharge plasma spectrum of air is dominated by O atoms and N ions, as shown in figure 7(c).

The precise control of the discharge plasma in time makes it possible to investigate the temporal evolution of the plasma. Therefore, we further measured the temporally resolved spectra of the discharge plasma in SF_6. In this case, we changed the gate width of the spectrometer to 100 ns to improve the temporal resolution. Figure 8 shows the decay of

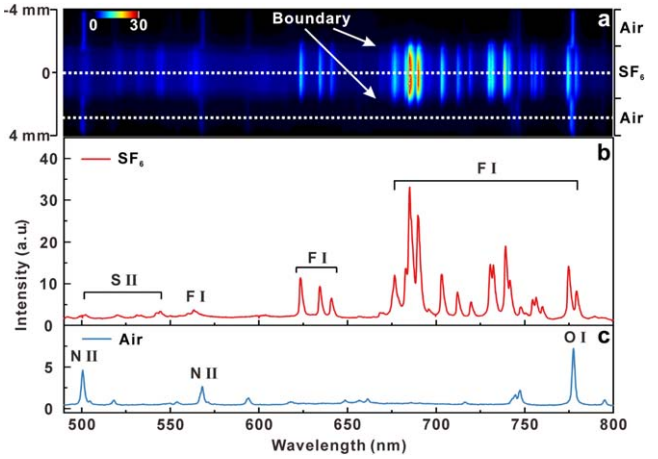

Figure 7. (a) Image of one-dimensional spatially resolved spectrum of flow field, (b) discharge plasma spectrum of SF_6, (c) discharge plasma spectrum of air.

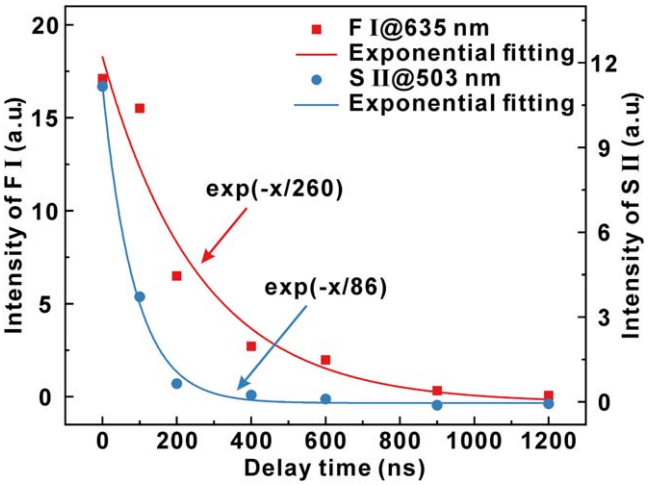

Figure 8. Decay of spectral intensities of F atom at 635 nm and S ion at 503 nm.

the spectral intensities of the F atom at 635 nm and the S ion at 503 nm. The exponential decay function was used to fit the data, and the lifetimes of F atom at 635 nm and S ion at 503 nm are 260 ns and 86 ns, respectively.

The experimental results show that the discharge plasma is spatially distributed along the filament and is precisely controlled by the filament in time. Hence, the spectra of the discharge plasma can be measured with a high spatial and temporal resolution by an imaging spectrometer. The spatio-temporally resolved spectra of the discharge plasma triggered by fs laser filament demonstrate the potential for one-dimensional composition measurements of gas flow fields. It also provides an effective technical method for studying the spatiotemporal evolution of discharge plasma.

4. Conclusion

This work investigated fs laser filament triggered and guided high-voltage DC pulse discharge. First, the spatial and temporal

control of the discharge triggered by fs filament was studied. In space, the discharge plasma is routed along the channel generated by fs laser filament. The fs laser filament lowers the gas breakdown voltage and dramatically extends the spatial length of the discharge plasma. In time, the effect of electrical parameters, e.g. the time interval between the filament and the voltage, the electrode voltage, and the electrode gap on discharge delay time and the jitter was investigated. A shorter discharge delay time can be obtained at a higher voltage and a shorter gap. The discharge breakdown inception can be controlled by adjusting only the time interval. It is preferable to directly generate the laser filament in an electric field to reduce the discharge jitter. Optimization of the electrical parameters enables precise control of the discharge time on the order of sub-nanoseconds.

Then, the feasibility of fs laser filament-triggered discharge in gaseous flow fields diagnostic applications was investigated. The controlled discharge plasma combined with optical emission spectroscopy is applied to measure the one-dimensional composition of a gas flow field. The one-dimensional temporally and spatially resolved spectra of the discharge plasma in SF_6 were obtained. In addition, the lifetimes of different spectral lines in the discharge plasma were calculated. The results demonstrate that fs laser filament-triggered discharge can achieve one-dimensional composition measurements of flow fields. It is also helpful for the study of the spatiotemporal evolution of discharge plasma.

Acknowledgments

This work was funded by National Natural Science Foundation of China (NSFC) (Nos. 51806149, 91741205).

References

[1] Tie W H *et al* 2018 *Plasma Sci. Technol.* **20** 014009
[2] Kosarev I N *et al* 2013 *Plasma Sources Sci. Technol.* **22** 045018
[3] Zheng D F 2016 *Plasma Sci. Technol.* **18** 1110
[4] Kuwabara A, Kuroda S I and Kubota H 2006 *Plasma Sources Sci. Technol.* **15** 328
[5] Shao T *et al* 2018 *High Volt.* **3** 14
[6] Yoshida K, Rajanikanth B S and Okubo M 2009 *Plasma Sci. Technol.* **11** 327
[7] Graves D B 2014 *Phys. Plasmas* **21** 080901
[8] Gallimberti I *et al* 2002 *C. R. Physique* **3** 1335
[9] Bruggeman P J, Iza F and Brandenburg R 2017 *Plasma Sources Sci. Technol.* **26** 123002
[10] Fridman A, Chirokov A and Gutsol A 2005 *J. Phys. D: Appl. Phys.* **38** R1
[11] Kojima H *et al* 2016 *IEEE Trans. Dielectr. Electr. Insul.* **23** 194
[12] Seeger M *et al* 2018 *IEEE Trans. Dielectr. Electr. Insul.* **25** 2147
[13] Nijdam S, Teunissen J and Ebert U 2020 *Plasma Sources Sci. Technol.* **29** 103001
[14] Lalande P *et al* 2002 *C. R. Physique* **3** 1375
[15] Dwyer J R and Uman M A 2014 *Phys. Rep.* **534** 147
[16] Larsson A 2012 *IEEE Trans. Plasma Sci.* **40** 2431
[17] Wang Q *et al* 2015 *IEEE Trans. Compon. Packag. Manuf. Technol.* **5** 460
[18] Couairon A and Mysyrowicz A 2007 *Phys. Rep.* **441** 47
[19] Bergé L *et al* 2007 *Rep. Prog. Phys.* **70** 1633
[20] Brelet Y *et al* 2012 *Appl. Phys. Lett.* **100** 181112
[21] Miki M and Wada A 1996 *J. Appl. Phys.* **80** 3208
[22] Arantchouk L *et al* 2016 *Appl. Phys. Lett.* **108** 173501
[23] Tzortzakis S *et al* 2001 *Phys. Rev.* E **64** 057401
[24] Forestier B *et al* 2012 *AIP Adv.* **2** 012151
[25] Clerici M *et al* 2015 *Sci. Adv.* **1** e1400111
[26] Schmitt-Sody A *et al* 2017 *AIP Adv.* **7** 035018
[27] Arantchouk L *et al* 2014 *J. Appl. Phys.* **116** 013303
[28] Arantchouk L *et al* 2014 *Appl. Phys. Lett.* **104** 103506
[29] Tamošauskas G *et al* 2005 *Lith. J. Phys.* **45** 37
[30] Luther B M *et al* 2001 *Appl. Phys. Lett.* **79** 3248
[31] Arantchouk L *et al* 2013 *Appl. Phys. Lett.* **102** 163502
[32] Li B *et al* 2018 *Opt. Express* **26** 21132
[33] Kosareva O G *et al* 2021 *Appl. Phys. Lett.* **119** 041103
[34] Zhao X M *et al* 1995 *IEEE J. Quantum Electron.* **31** 599
[35] Papeer J *et al* 2019 *Sci. Rep.* **9** 407
[36] Produit T *et al* 2021 *Eur. Phys. J. Appl. Phys.* **93** 10504
[37] Brussaard G J H and Hendriks J 2005 *Appl. Phys. Lett.* **86** 081503
[38] Brussaard G J H and Hendriks J 2007 *IEEE Trans. Dielectr. Electr. Insul.* **14** 976
[39] Brelet Y *et al* 2012 *Appl. Phys. Lett.* **101** 264106
[40] Théberge F *et al* 2017 *Appl. Phys. Lett.* **111** 073501
[41] Rosenthal E W *et al* 2020 *Opt. Express* **28** 24599
[42] Tzortzakis S *et al* 2000 *Opt. Commun.* **181** 123
[43] Li H *et al* 2019 *Plasma Sci. Technol.* **21** 074008